esteem3

Enabling Science through European Electron Microscopy

Report onquantitative chemical atomic resolution mapping

Deliverable D5.3 – version 1.1

Estimated delivery date:	M52, April, 30th 2023
Actual delivery date:	M53, May 4th, 2023
Lead beneficiary:	TUGraz
Person responsible:	Gerald Kothleitner
Deliverable type:	☒ R ☐ DEM ☐ DEC ☐ OTHER ☐ ETHICS ☐ ORDP
Dissemination level:	☒ PU ☐ CO ☐ EU-RES ☐ EU-CON ☐ EU-SEC

THIS PROJECT HAS RECEIVED FUNDING FROM THE EUROPEAN UNION'S HORIZON 2020 RESEARCH AND INNOVATION PROGRAMME UNDER GRANT AGREEMENT NO **823717**

Grant Agreement No:	823717
Funding Instrument:	Research and Innovation Actions (RIA)
Funded under:	H2020-INFRAIA-2018-1: Integrating Activities for Advanced Communities
Starting date:	01.01.2019
Duration:	54 months

Table of contents

Revision history log

Version number	Date of release	Author	Summary of changes
V0.1	April 16th 2023	Gerald Kothleitner	Preparation of the initial version of the report
V0.2	April 17th 2023	Rafal E. Dunin-Borkowski	Corrections
V1.0	May 3rd, 2023	Peter A. van Aken	Approval
V1.1	May 4th, 2023	Lucie Guilloteau	Editing

Introduction

Knowing where the atoms are, what the atoms are and how they are bonded are fundamental questions connected to the analysis of any modern material. As chemical compositions and atomic structural arrangements ultimately drive their properties and functionalities, reliable pathways to explore elemental occurrences in a quantitative manner are key. Generally, in (scanning) transmission electron microscopy (S)TEM several approaches exist to address the questions of material compositions, offering differing capabilities and requiring changing analysis procedures. These are on one hand suitable imaging modes, whereby elastic signal modalities of a kind can be turned into concentrations via comparisons or normalizations to simulations. Or, by contrast, harnessing inelastic interactions of electrons with matter, leading to energy-losses of the primary electron beam and secondary X-rays, with the respective spectroscopies named electron energy-loss spectroscopy (EELS) and energy dispersive X-ray spectroscopy (EDXS). Even though inelastic analysis concepts have been established for studies at the micrometer to nanometer scale a while ago, an absolute scale quantification of inelastic data at the atomic level remains elusive until today. Most of the complications originate from the physics of the electron beam interaction with the specimen in a zone axis orientation and the resulting signals, from fundamental uncertainties in the proportionality factors needed to turn intensities into concentrations, or from the need for accompanying simulations that often require a priori knowledge about an unknown, to-be-determined structure that potentially contains defects. The report aims to review the issues, summarizes the findings within the project, and gives an assessment of possible solutions.

Dynamic scattering

Figure 1 of this report shall act as a starting point to illustrate briefly some of the fundamental phenomena that occur, when a pencil-type STEM probe transmits a single crystal material along a low index zone-axis.

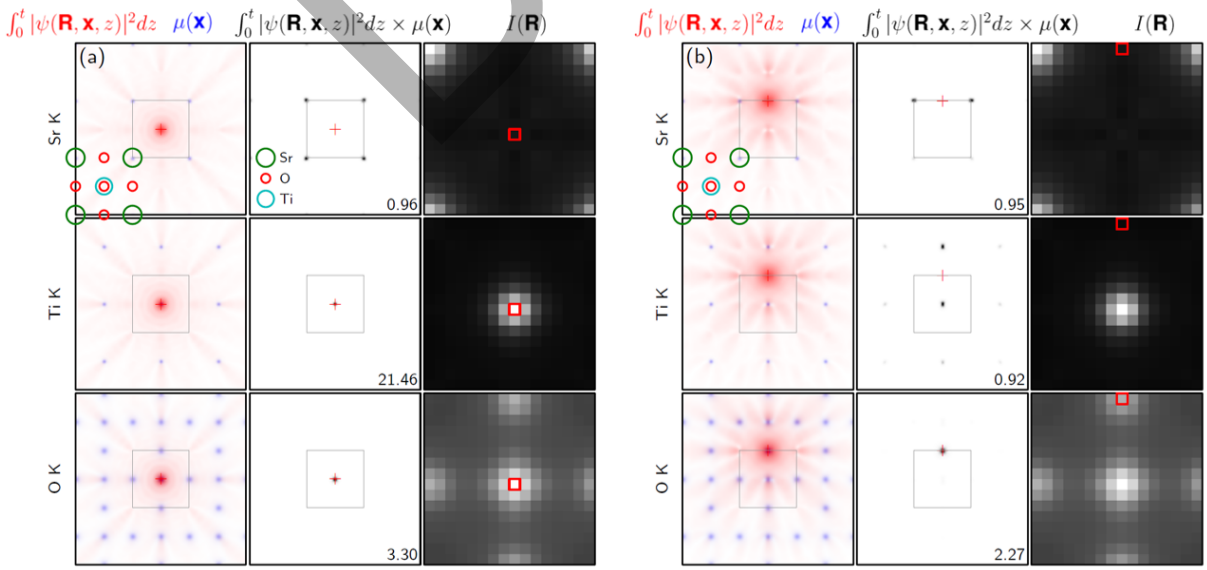

Figure 1: Depth- integrated probe intensities and inelastic potentials for various probe positions in the Sr-K, Ti- K and O-K lines of strontium titanate (STO) (left) on a mixed Ti/O column and (right) at a pure O column [from 1].

Within each panel, three different columns are visible that have been obtained with simulations carried out with µSTEM code. In red the propagation and scattering of a 200 kV, aberration-corrected STEM electron beam with a convergence angle of 22 mrad is displayed, traveling through a ~ 60 nm thick area of STO. The red cross thereby indicates the beam position. The square denotes the location of the unit cell (structure on the left), whereas the blue dots represent the ionization probabilities of the elements Sr-K, Ti-K and O-K. The second column shows the overlap product of these two functions, with the averaged intensity (over an 8x8 unit cell area and expressed in terms of the deviation from non-channeling signal) written in the lower right corner. On the right column, the resulting EDXS STEM map is given for a single unit cell with the pixel indicating the probe position.

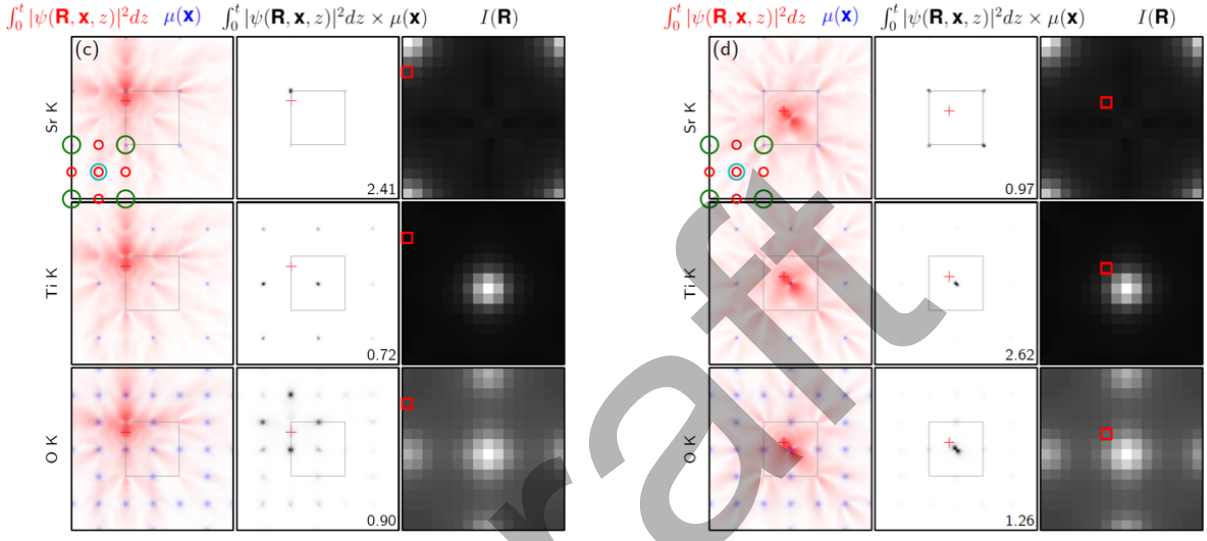

Figure 2: (left) Situation of the probe near the Sr column and (right) near the Ti/O column [from 1].

In figure 1, the probe is directly on top of atomic columns from Ti/O in the first case and a pure O column in the second. In both cases, the probe is concentrated at the columns, however, in the case of the Ti/O column, the probe is more strongly attracted to the column, whereas on the pure O site electrons strongly propagate away from the beam position. The second two probe positions in figure 2 are slightly displaced from the Sr and Ti/O columns. In these cases, even though the probe is not directly positioned above a column, it gets attracted to, and scattered away from that column. In all circumstances, the (red) electron beam overlaps to different degrees with the potentials, ultimately leading to different amounts of extra signal ascribed to the original beam position intensity. Depending on the crystal structure and the atomic number of the elements that make up the unit cell, inelastic intensities inevitably yield incorrect concentration numbers imposed by the physics of the dynamic scattering.

The picture describes what is long known as the channeling and de-channeling of electrons in the crystal field of a specimen. For atomic resolution imaging, electron channeling is beneficial, since it enables the focusing of a beam down an atomic column, producing enhanced signals with high contrast, such as for Rutherford scattering and high-angle annual dark-field images. For a reliable quantitative analysis based on X-rays or EELS signal, however, one ought to operate under kinematical conditions and stay away from any bend centers or bend contours – a situation often not applicable when atom counting is envisioned.

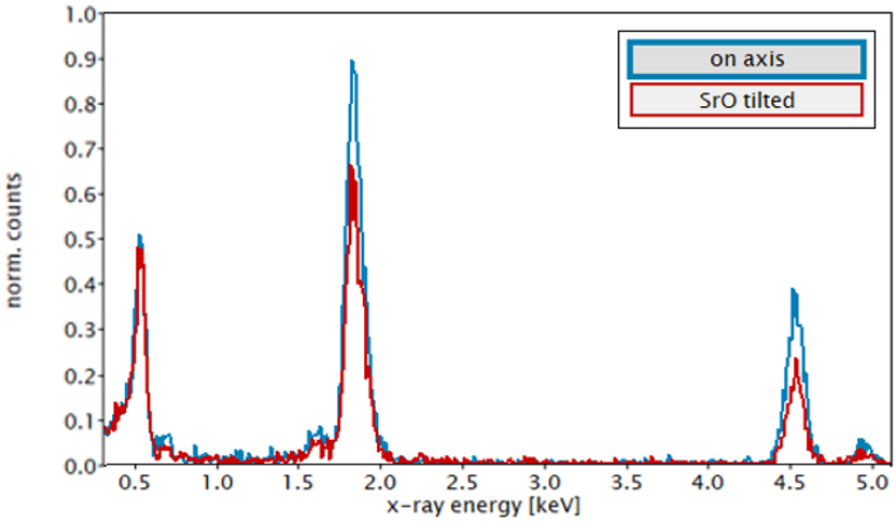

Figure 3: X-ray spectra from STO taken on-axis [100] and under slightly tilted conditions.

It shall be noted that the signal enhancement leading to an enhanced X-ray emission compared with kinematical conditions can sometimes be used to locate, which atoms lie on which crystal planes - a technique (mostly ignored these days) referred to as ALCHEMI. This effect can be seen in figure 3 and makes clear that common analysis schemes such as the Cliff-Lorimer or the ζ-factor approach (zeta factor) in EDXS [2], which assume constant emission with specimen tilt, are violated. Similar considerations hold for a quantitative EELS analysis, albeit the differences in the signal itself.

Quantitative chemical composition analysis with EDXS and EELS– the fundamentals

For a better understanding of the conversion path in EDXS and EELS from recorded intensities to concentrations, a few equations shall be given. They show the connections between the respective techniques but also reveal the potential for synergistic use of a simultaneous heavy and light element analysis, which X-ray and EELS are representing. For EDXS the starting point is the ζ-factor approach [2], which has some advantages because of an intrinsic absorption correction.

$$\rho \times t = \zeta \frac{I^X}{D} \qquad \rho \times t = \zeta_A \frac{I_A^X A_A}{C_A D} \qquad \zeta_A = \zeta_B \frac{I_B^X A_B C_A}{I_A^X A_A C_B} \tag{1}$$

$$\rho \times t = \frac{I^E}{I_0^E \sigma} \times \frac{AW}{N_{AV}} \tag{2}$$

$$\zeta \times \sigma = \frac{I^E}{I_0^E I^X} \times \frac{AW}{N_{AV}} \times D \tag{3}$$

$$\frac{\zeta_A}{\zeta_B} \times \frac{\sigma_A}{\sigma_B} = \frac{I_B^X}{I_A^X} \times \frac{A_B}{A_A} \times \frac{I_A^E}{I_B^E} \times \frac{AW_A}{AW_B} \tag{4}$$

Figure 4: Mathematical framework for a EDXS and EELS compositional analysis

For a pure element in EDXS (line 1), mass-thickness (ρ*t) is linked via the ζ-factor to the ratio of the observed X-ray intensity (I^X), and the dose (D). The other equations are for an element in a compound, with concentration C and possible X-ray absorption A (middle), and for the relation of the ζ-factors in a binary compound (right). In EELS (line 2), the mass-thickness can be expressed as the core loss-intensity I^E normalized by the corresponding low-loss integral I^E_0 and inner-shell ionization cross-section σ multiplied by the ratio of the atomic weight AW and Avogadro´s number N_{AV}. From these equations, it becomes clear that the analytical intensities from EELS and EDXS, measured in one run under identical conditions, serve to yield the product $\zeta * \sigma$ when normalized by two constants (the atomic weight AW and Avogadro´s number N_{AV}) and considering the dose D. Explicitly, the product of the ζ-factor and the EELS cross-section σ can be expressed through line (3), and for a compound through line (4).

The table shows that a simultaneous measurement of EDXS and EELS intensities and of the dose, allows for easy conversion of one into the other. It should be emphasized that the power of light element EELS analysis can be used to populate ζ-factors for light elements in EDX, often hard to determine otherwise. Conversely, EDX ζ-factors, easy to calibrate for heavier elements, can be turned into EELS cross-sections even for edges, where theoretical cross-section models are complicated (M, N, O edges). Unfortunately, however, this linkage also rather clearly illustrates the dependencies of all factors from the intensities affected by the dynamic scattering.

In general, it became rather evident in the project within WP5 and WP7 that -whenever possible- a simultaneous acquisition strategy shall be targeted, offering the most information gain and flexibility for chemical analysis. This strategy, however, inevitably must be accompanied by endeavours to understand and tackle the influence of beam propagation and to minimize its impact. In addition, ideas to timely delineate energy-losses and X-ray events [8] have also helped to make quantification more accessible. These achievements are outlined in other deliverables for example in D5.4.

Possibilities to handle dynamic scattering effects

Simulation assisted studies

In cases of large compositional changes in the elemental distribution from column to column and favorable crystal structures, dynamical scattering simulations can be added to an analysis. In WP5 work by Lammer [3], a procedure was developed to determine the concentration of two elements within equivalent atomic columns from EELS elemental maps. In a second order Ruddlesden-Popper phase, relevant in electrochemical and energy applications, the barium and lanthanum concentrations within the A-sites of $Ba_{1.1}La_{1.9}Fe_2O_7$ compound have been evaluated.

For this, contributions from on-axis atoms (i.e., at the beam position) and off-axis atoms (i.e., in nearest-neighbour or next-nearest-neighbour columns) were evaluated separately. The counting necessitates the on-axis atoms (approximate) removal of any non-local, off-axis contribution from the experimental signal. This approximately accounts for the amount of artefact intensity caused by the electron scattering processes). In order to gauge these contributions on the elastic scattering, different site-specific elemental loadings, represented by the Ba M_{45} (781 eV) and the La M_{45} (832 eV) edges, have been simulated via inelastic multi-slice simulations. In this manner, a comparison of the origin of

the signal from both elements became possible and the behaviour between A-positions in the perovskite layer and in the rock salt layer of the structure could be distinguished. That way, a simple channelling correction mechanism for the experimental data by subtracting a certain amount of the average-unit-cell-intensity from the measured data was embedded and helped to get the Ba / La occupancies in each atomic column. It has to be noted that such a correction is valid for a certain sample thickness only and cannot be applied in general.

Of more general applicability, however, is the procedure developed for the determination of column concentrations. In short first, the channelling corrected intensities are connected with a newly introduced factor that entails the EELS cross-sections σ for the signals, yet avoiding their explicit knowledge. Subsequently, a Voronoi cell based statistical scatter plot analysis directly reveals the clustering of certain La/Ba ratios at atomic sites together with quantitative information obtained from the slope and intercept. Further details are given in the paper [3].

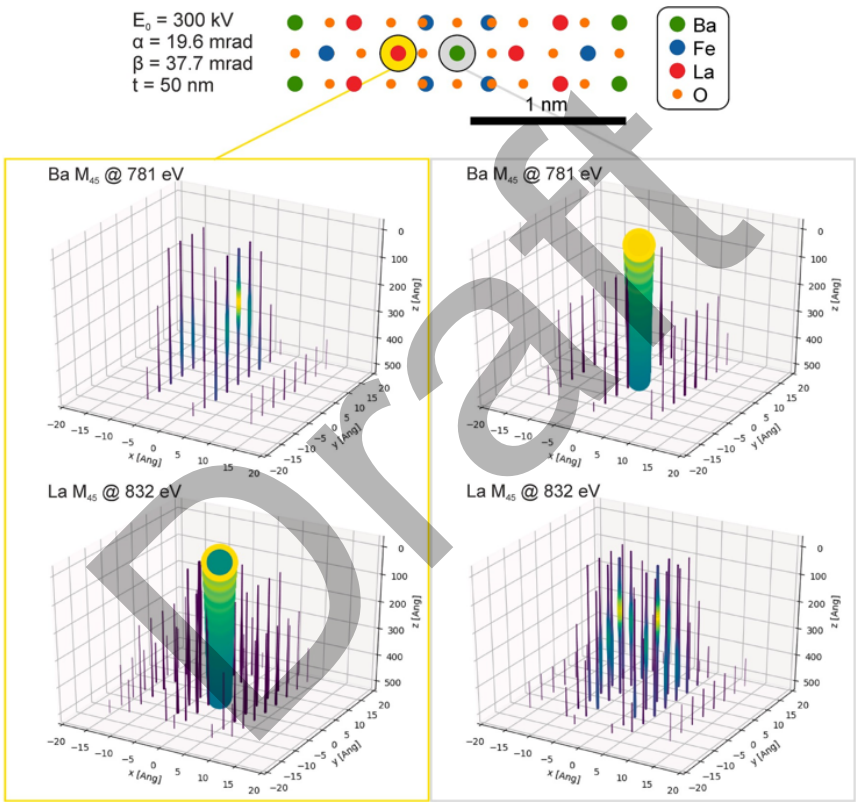

Figure 5: Inelastic multislice calculations for 2 beam positions in a second order Ruddlesden-Popper phase. La on rocksalt layer (yellow, left) and Ba on perovskite layer (grey, right). Extra contributions from neighboring sites to signal were evaluated (from [3]).

Another different methodology, pioneered by the groups in Oxford and Antwerp, is based on the combination of EDXS and high-angle annular dark field (HAADF) scanning transmission electron microscopy. In a recent ESTEEM publication [4], metallic nano-structures such as an Au@Ag core–shell nanorod, which are interesting because of their unique electronic, optical, or catalytic properties, have been investigated. The approach expands on the above principle, describing intensities as the overlap integral of a projected potential and the probe electron density.

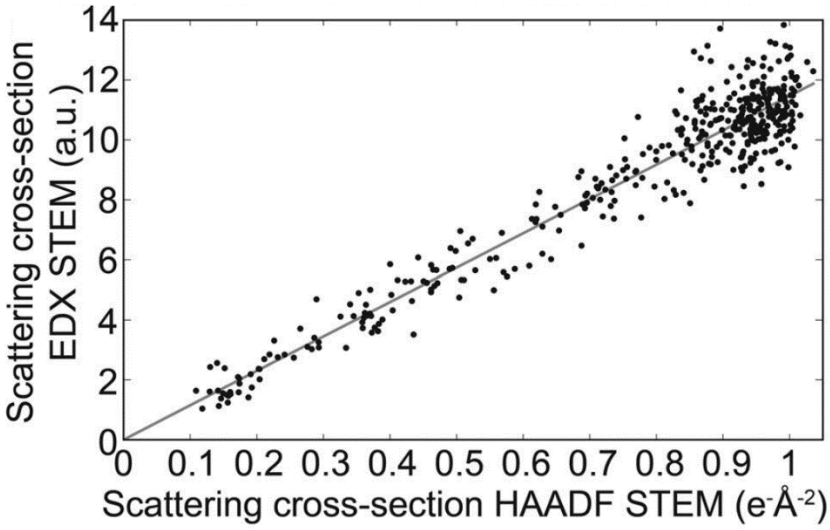

Figure 6: *EDX STEM scattering cross-sections as a function of the HAADF STEM scattering cross-sections. The line shows the linear relationship between the scattering cross-sections of both techniques for Ce-L in a CeO_2 nanoparticle (from [4]).*

In this case, it was shown that a linear relationship between the TDS absorptive (for HAADF) and effective ionization potential (for EDXS) can be expected and thus the monotonic increase of the scattering cross-section with thickness can be used to count the number of atoms in a column.

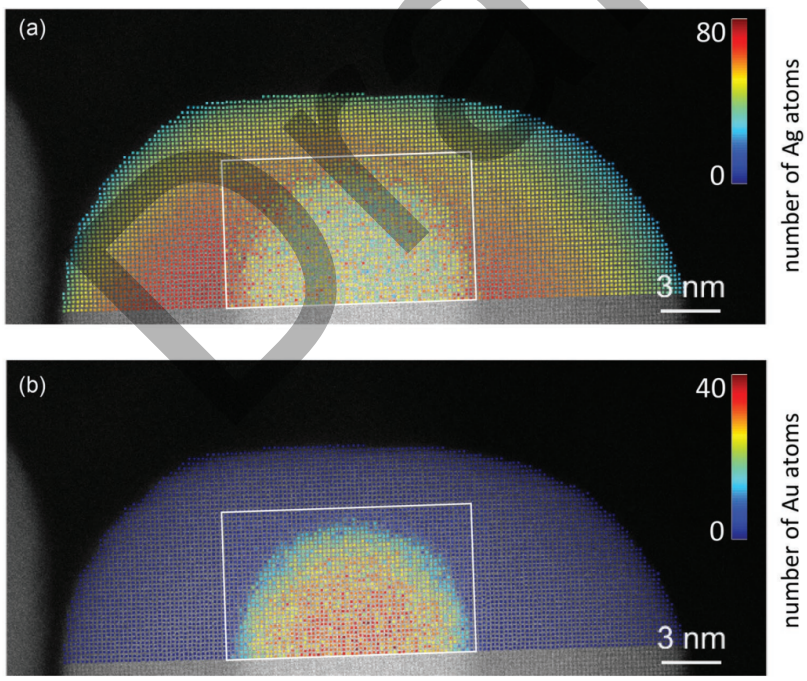

Figure 7: *EDX STEM scattering cross-sections as a function of the HAADF STEM scattering cross-sections. The line shows the linear relationship between the scattering cross-sections of both techniques for Ce-L in a CeO_2 nanoparticle (from [4]).*

This novel methodology can also be applied to materials systems, in which elements have almost identical atomic numbers, thus opening up new opportunities for the analysis of a wide variety of multi-metallic nanocrystals.

An important aspect that has to be considered in atomic resolution elemental analysis is the effect of beam dose to the specimen, potentially leading to damage, vacancy introduction and mass loss. The small cross-sections associated with inelastic imaging often result in high-dose acquisition strategies to obtain signals high enough to be subject to quantitative analysis. For this reason, noise filtering procedures by principal components analysis and acquisitions via high-DQE (EELS) / high collection efficiency detectors (EDXS) have turned out being beneficial throughout the WPs and have been used to the largest extent possible. At the same time, novel STEM strategies have been worked on that aimed at a reduction of dose-accumulation effects. The acquisition of random sparse images combined with the capability of reconstructing the target image with adapted post-processing techniques has emerged as an efficient way to reduce total electron dose and dose accumulation effects [5,6,7].

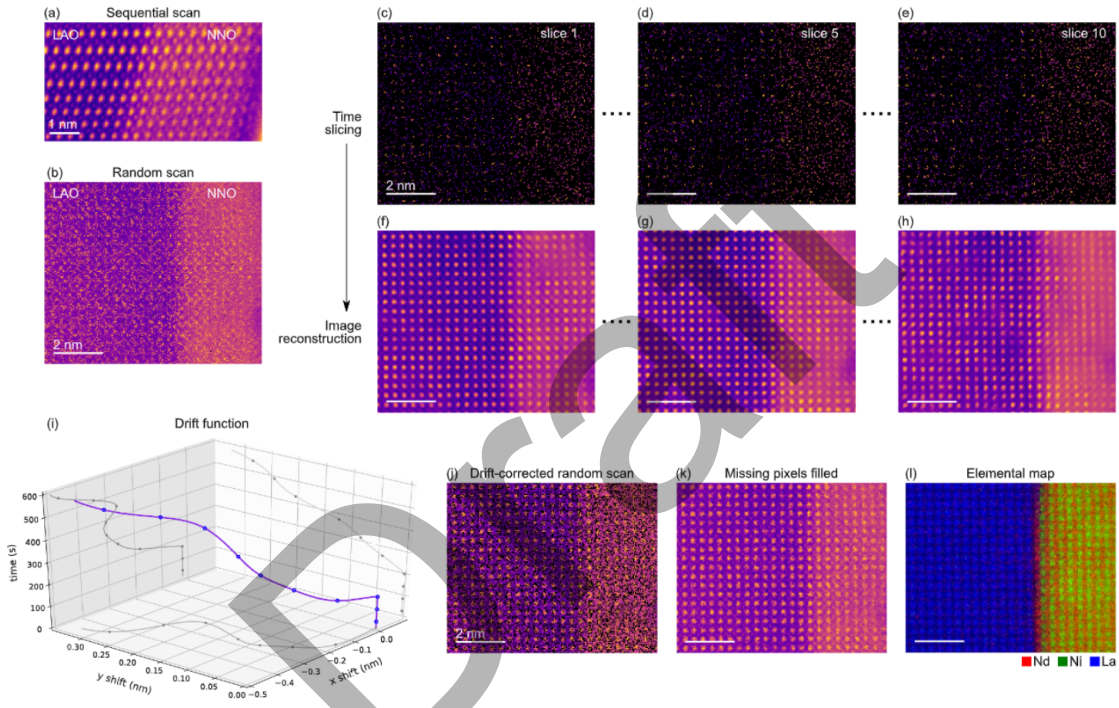

Figure 8: STEM-HAADF image of the $NdNiO_3$–$LaAlO_3$ (NNO–LAO) interface acquired (a) in the standard sequential raster scan mode and (b) in the random scan mode. Atomically resolved EELS spectrum images (i) can be reconstructed after processing (c-k) (from [5]).

Further research related to questions of an atomic level analysis incorporated results from other spectroscopic techniques to provide additional, indirect support of specific situations in diverse material systems. These are CL, XPS, Raman, electrical resistivity measurements or similar [refs > 8]. Also, other imaging techniques such as iDPC being more sensitive to light elements are likely to contribute.

Despite the power of correlative work-flows, however, ultimately innnovations to the microscope scan engines at the hardware level that yield more flexibility have been identified as a major bottleneck. Faster scan times, a much-improved beam movement manipulation and generally higher degrees of freedom for beam stirring at the microsecond range or even shorter, while maintaining atomic resolution, will alleviate current limitations of STEM imaging – as will be outlined next.

"Kinematic" spectroscopy

Fundamentally, a tilted electron probe (or likewise a specimen tilted out of zone-axis) starts matching a free-space propagating probe. This assessment comes with the observation that conditions of "kinematic character" tend to reduce the problems of enhanced or reduced inelastic intensities in spectroscopy.

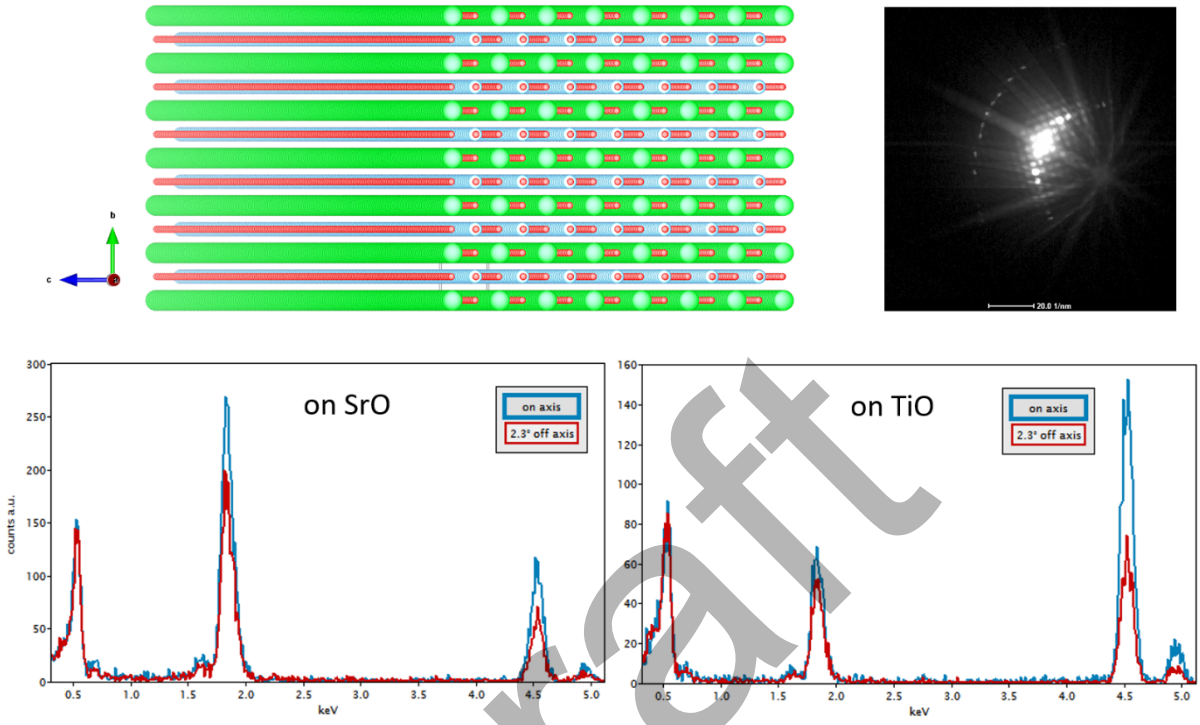

Figure 9: (upper left) STO specimen tilted ~ 2° away from zone axis and (upper right) diffraction pattern becoming more kinematic. (below) changing EDXS spectral intensities as a function of tilt and atom position (at Sr or at Ti/O layer) [unpublished results].

A series of inelastic STEM images tilted to different angles should become intrinsically better quantifiable. In this light, a STEM beam precessing around a few degrees at every pixel position would strongly reduce the effects of channelling and dynamic diffraction. The use of this technique has been extensively studied in diffraction pattern analyses at a lower scale. At the atomic level spatial information will get averaged out and contrast drops. Nevertheless, atomic resolution information along different directions will be maintained with the benefit that the average of such images enhances the accuracy of the data for more faithful numbers.

Technologically, the method of beam precession has not yet been developed to a point where these experiments are possible at the spatial resolution needed. From the project, it became clear however, that this type of data acquisition needs to be enforced – along with some changes outlined before. Talks and negotiations with STEM column and OEM vendors about more powerful implementations are already on the way. One issue that needs to be overcome is the conflict of precession angle and spatial resolution, something that requires aberration correctors of a new kind. Only wide-angle acceptance aberration modules will be able to keep the beam aberrations at a minimum, so that a kinematic, atomic-level analysis becomes possible. With the next generation STEM microscopes around the corner, one can expect to see improvements in this specific application soon.

Summary

One aspect in WP5, and the topic in this deliverable, was the question of determining elemental compositions at the atomic scale accurately. In a nutshell, the problem that needs to be overcome is the dynamical scattering of the electron beam, which becomes significant for realistic TEM specimen thicknesses at between 20 and 50 nm. As it stands, image simulations that estimate these effects for known structures can assist the corrections needed to convert false inelastic signal intensities. Incorporating other imaging modalities and connecting them with spectroscopies also shows promise for the analysis of certain material systems. Complicated structures, containing defects and vacancies, however, impose further far-reaching challenges to STEM techniques. The largest prospects currently seem to lie in improved beam management. This can not only alleviate dose issues but potentially also delivers more "kinematic" data. Alongside this, the importance of high-quality thin specimen lamellae preparation cannot be emphasized enough.

References

Publications

[1] Lugg, N. R., Kothleitner , G., Shibata, N. ,and Ikuhara Y. "On the quantitativeness of EDS STEM." Ultramicroscopy 151 (2015) 150. http://dx.doi.org/10.1016/j.ultramic.2014.11.029.

[2] Watanabe, M., Williams, D. "The quantitative analysis of thin specimens: a re- view of progress from the Cliff-lorimer to the new ζ-factor methods, J. Microsc. 221 (2) (2006) 89–109. http://dx.doi.org/10.1111/j.1365- 2818.2006.01549.x.

[3] Lammer, J, C Berger, S Löffler, D Knez, P Longo, G Kothleitner, F Hofer, et al. "A Method for a Column-by-Column EELS Quantification of Barium Lanthanum Ferrate." Ultramicroscopy 234 (2022). https://doi.org/10.1016/j.ultramic.2022.113477.

[4] Backer, Annick De, Zezhong Zhang, Karel H.W. van den Bos, Eva Bladt, Ana Sánchez-Iglesias, Luis M. Liz-Marzán, Peter D Nellist, Sara Bals, and Sandra Van Aert. "Element Specific Atom Counting at the Atomic Scale by Combining High Angle Annular Dark Field Scanning Transmission Electron Microscopy and Energy Dispersive X-ray Spectroscopy." Small Methods 6, no. 11 (November 30, 2022): 2200875. https://doi.org/10.1002/smtd.202200875.

[5] Zobelli, A., Woo, S.Y., Tararan, A., Tizei, L.H.G., Brun, N., Li, X., Stéphan, O., Kociak, M., Tencé, M. "Spatial and spectral dynamics in STEM hyperspectral imaging using random scan patterns." Ultramicroscopy 212 (2020) 112912, https://doi.org/10.1016/j.ultramic.2019.112912.

[6] Jannis, D, A Velazco, A Béché, and J Verbeeck. "Reducing Electron Beam Damage through Alternative STEM Scanning Strategies, Part II: Attempt towards an Empirical Model Describing the Damage Process." Ultramicroscopy 240 (2022). https://doi.org/10.1016/j.ultramic.2022.113568.

[7] Velazco, A, A Béché, D Jannis, and J Verbeeck. "Reducing Electron Beam Damage through Alternative STEM Scanning Strategies, Part I: Experimental Findings." Ultramicroscopy 232 (2022). https://doi.org/10.1016/j.ultramic.2021.113398.

[8] Jannis, D, K Müller-Caspary, A Béché, and J Verbeeck. "Coincidence Detection of Eels and Edx Spectral Events in the Electron Microscope." Applied Sciences (Switzerland) 11, no. 19 (2021). https://doi.org/10.3390/app11199058.

Further References with respect to this work (unordered)

Zobelli, A; Woo, SY; Tararan, A; Tizei, LHG; Brun, N; Li, XY; Stephan, O; Kociak, M; Tencee, M Spatial and spectral dynamics in STEM hyperspectral imaging using random scan patterns ULTRAMICROSCOPY http://dx.doi.org/10.1016/j.ultramic.2019.112912

Krishnia, S; Haltz, E; Berges, L; Aballe, L; Foerster, M; Bocher, L; Weil, R; Thiaville, A; Sampaio, J; Mougin, A Spin-Orbit Coupling in Single-Layer Ferrimagnets: Direct Observation of Spin-Orbit Torques and Chiral Spin Textures PHYSICAL REVIEW APPLIED http://dx.doi.org/10.1103/PhysRevApplied.16.024040

Teurtrie, A; Popova, E; Koita, I; Chikoidze, E; Keller, N; Gloter, A; Bocher, L Atmosphere-Induced Reversible Resistivity Changes in Ca/Y-Doped Bismuth Iron Garnet Thin Films ADVANCED FUNCTIONAL MATERIALS http://dx.doi.org/10.1002/adfm.201904958

Teurtrie, A; Bocher, L; Mougin, A; Keller, N; Gloter, A; Popova, E Evolution of structural and magnetic properties of multifunctional bismuth iron garnets upon Ca and Y doping PHYSICAL REVIEW MATERIALS http://dx.doi.org/10.1103/PhysRevMaterials.4.064401

Atomic-scale determination of cation and magnetic order in the triple perovskite Sr3Fe2ReO9
P-L Ho, Z Huang, L Jin, S-Y Choi, R E Dunin-Borkowski, J Mayer, F-R Chen, S C E Tsang, P D Nellist and X Zhong Microsc. Microanal. 29 (2023), 326-333.
https://doi.org/10.1093/micmic/ozac011
Li, XY; Zhu, QX; Vistoli, L; Barthelemy, A; Bibes, M; Fusil, S; Garcia, V; Gloter, A In-Depth Atomic Mapping of Polarization Switching in a Ferroelectric Field-Effect Transistor ADVANCED MATERIALS INTERFACES http://dx.doi.org/10.1002/admi.202000601

Gloter, A; Tieri, G; Li, DF; Caputo, M; Strocov, VN; Stephan, O; Triscone, JM; Gariglio, S Role of point and line defects on the electronic structure of LaAlO3/SrTiO3 interfaces APL MATERIALS http://dx.doi.org/10.1063/1.5132376

Ismail, ASM; Casavola, M; Liu, BY; Gloter, A; van Deelen, TW; Versluijs, M; Meeldijk, JD; Stephan, O; de Jong, KP; de Groot, FMF Atomic-Scale Investigation of the Structural and Electronic Properties of Cobalt-Iron Bimetallic Fischer-Tropsch Catalysts ACS CATALYSIS http://dx.doi.org/10.1021/acscatal.8b04334

Fusil, S; Chauleau, JY; Li, XY; Fischer, J; Dufour, P; Leveille, C; Carretero, C; Jaouen, N; Viret, M; Gloter, A; Garcia, V Polar Chirality in BiFeO3 Emerging from A Peculiar Domain Wall Sequence ADVANCED ELECTRONIC MATERIALS http://dx.doi.org/10.1002/aelm.202101155

Tovani, CB; Oliveira, TM; Soares, MPR; Nassif, N; Fukada, SY; Ciancaglini, P; Gloter, A; Ramos, AP Strontium Calcium Phosphate Nanotubes as Bioinspired Building Blocks for Bone Regeneration ACS APPLIED MATERIALS & INTERFACES http://dx.doi.org/10.1021/acsami.0c12434

Lee, JH; Marcano, L; Aeschlimann, R; Mawass, MA; Luo, C; Gloter, A; Varignon, J; Radu, F; Valencia, S; Bibes, M Strain tuning of Neel temperature in YCrO3 epitaxial thin films APL MATERIALS http://dx.doi.org/10.1063/5.0095742

Monier, E., Oberlin, T., Brun, N., Li, X., Tencé, M., & Dobigeon, N. (2020). Fast reconstruction of atomic-scale STEM-EELS images from sparse sampling. Ultramicroscopy, 112993. https://doi.org/10.1016/j.ultramic.2020.112993

Huang, Yuanye, Rotraut Merkle, Dan Zhou, Wilfried Sigle, Peter A. van Aken, and Joachim Maier. “Effect of Ni on Electrical Properties of Ba(Zr,Ce,Y)O3-δ as Electrolyte for Protonic Ceramic Fuel Cells.” Solid State Ionics 390, no. November 2022 (2023): 116113. https://doi.org/10.1016/j.ssi.2022.116113.

Nono Tchiomo, Arnaud P., Emanuela Carleschi, Aletta R.E. Prinsloo, Wilfried Sigle, Peter A. Van Aken, Jochen Mannhart, Prosper Ngabonziza, and Bryan P. Doyle. "Combined Spectroscopy and Electrical Characterization of La:BaSnO3thin Films and Heterostructures." AIP Advances 12, no. 10 (2022). https://doi.org/10.1063/5.0105116.

Ma, Tian, Hao Cao, Shuang Li, Sujiao Cao, Zhenyang Zhao, Zihe Wu, Rui Yan, et al. "Crystalline Lattice-Confined Atomic Pt in Metal Carbides to Match Electronic Structures and Hydrogen Evolution Behaviors of Platinum." Advanced Materials 34, no. 41 (2022): 1–11. https://doi.org/10.1002/adma.202206368.

Cheng, Pengfei, Joachim Döll, Henry Romanus, Hongguang Wang, Peter A. van Aken, Dong Wang, and Peter Schaaf. "Reactive Magnetron Sputtering of Large-Scale 3D Aluminum-Based Plasmonic Nanostructure for Both Light-Induced Thermal Imaging and Photo-Thermoelectric Conversion." Advanced Optical Materials 11, no. 6 (March 26, 2023): 2202664. https://doi.org/10.1002/adom.202202664.

Elibol, Kenan, Toma Susi, Clemens Mangler, Dominik Eder, Jannik C. Meyer, Jani Kotakoski, Richard G. Hobbs, Peter A. van Aken, and Bernhard C. Bayer. "Linear Indium Atom Chains at Graphene Edges." Npj 2D Materials and Applications 7, no. 1 (2023): 1–8. https://doi.org/10.1038/s41699-023-00364-6

Harbola, Varun, Yu Jung Wu, Hongguang Wang, Sander Smink, Sarah C. Parks, Peter A. van Aken, and Jochen Mannhart. "Self-Assembly of Nanocrystalline Structures from Freestanding Oxide Membranes." Advanced Materials 35, no. 10 (2023). https://doi.org/10.1002/adma.202210989.

Zhao, Run, Chao Yang, Hongguang Wang, Kai Jiang, Hua Wu, Shipeng Shen, Le Wang, et al. "Emergent Multiferroism with Magnetodielectric Coupling in EuTiO3 Created by a Negative Pressure Control of Strong Spin-Phonon Coupling." Nature Communications 13, no. 1 (2022): 1–9. https://doi.org/10.1038/s41467-022-30074-4.

Yang, Chao, Yi Wang, Daniel Putzky, Wilfried Sigle, Hongguang Wang, Roberto A. Ortiz, Gennady Logvenov, Eva Benckiser, Bernhard Keimer, and Peter A. Van Aken. "Ruddlesden-Popper Faults in NdNiO3 Thin Films." Symmetry 14, no. 3 (2022): 1–9. https://doi.org/10.3390/sym14030464.

Wang, Hongguang, Gennadii Laskin, Weiwei He, Hans Boschker, Min Yi, Jochen Mannhart, and Peter A. van Aken. "Tunable Magnetic Anisotropy in Patterned SrRuO3 Quantum Structures: Competition between Lattice Anisotropy and Oxygen Octahedral Rotation." Advanced Functional Materials, 2022. https://doi.org/10.1002/adfm.202108475.

References of general relevance

Watanabe, M., Williams, D. "The quantitative analysis of thin specimens: a review of progress from the Cliff-Lorimer to the new ζ-factor methods, J. Microsc. 221 (2) (2006) 89–109. http://dx.doi.org/10.1111/j.1365- 2818.2006.01549.x

Watanabe, M, and R F Egerton. "Evolution in X-Ray Analysis from Micro to Atomic Scales in Aberration-Corrected Scanning Transmission Electron Microscopes." Microscopy 71 (2022): I132–47. https://doi.org/10.1093/jmicro/dfab026.

Egerton, R.F., Malac, M. "EELS in the TEM", Journal of Electron Spectroscopy and Related Phenomena, 143(2–3), 2005, 43-50, https://doi.org/10.1016/j.elspec.2003.12.009